



HAL
open science

A multi-omics concentration-response framework uncovers novel understanding of triclosan effects in the chlorophyte *Scenedesmus vacuolatus*

Floriane Larras, Elise Billoir, Stefan Scholz, Mika Tarkka, Tesfaye Wubet, Marie Laure Delignette-Muller, Mechthild Schmitt-Jansen

► To cite this version:

Floriane Larras, Elise Billoir, Stefan Scholz, Mika Tarkka, Tesfaye Wubet, et al.. A multi-omics concentration-response framework uncovers novel understanding of triclosan effects in the chlorophyte *Scenedesmus vacuolatus*. *Journal of Hazardous Materials*, 2020, 397, pp.122727. 10.1016/j.jhazmat.2020.122727 . hal-02892773

HAL Id: hal-02892773

<https://cnrs.hal.science/hal-02892773v1>

Submitted on 7 Jul 2020

HAL is a multi-disciplinary open access archive for the deposit and dissemination of scientific research documents, whether they are published or not. The documents may come from teaching and research institutions in France or abroad, or from public or private research centers.

L'archive ouverte pluridisciplinaire **HAL**, est destinée au dépôt et à la diffusion de documents scientifiques de niveau recherche, publiés ou non, émanant des établissements d'enseignement et de recherche français ou étrangers, des laboratoires publics ou privés.



A multi-omics concentration-response framework uncovers novel understanding of triclosan effects in the chlorophyte *Scenedesmus vacuolatus*

Floriane Larras^{a,*}, Elise Billoir^b, Stefan Scholz^a, Mika Tarkka^{c,d}, Tesfaye Wubet^{e,d}, Marie-Laure Delignette-Muller^f, Mechthild Schmitt-Jansen^{a,*}

^a Helmholtz-Centre for Environmental Research – UFZ, Department of Bioanalytical Ecotoxicology, Permoserstrasse 15, 04318 Leipzig, Germany

^b Université de Lorraine, CNRS, LIEC, F-57000 Metz, France

^c Department of Soil Ecology, Helmholtz-Centre for Environmental Research – UFZ, Theodor-Lieser-Straße 4, 06120 Halle, Germany

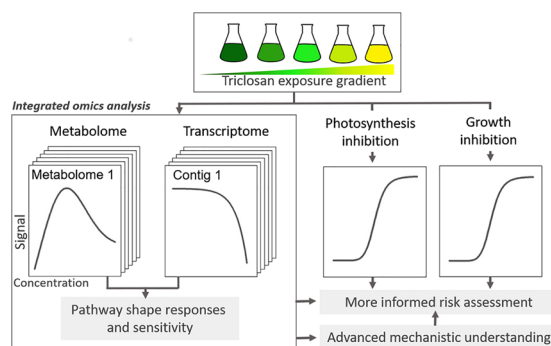
^d German Centre for Integrative Biodiversity Research (iDiv) Halle-Jena-Leipzig, Deutscher Platz 5e, 04103 Leipzig, Germany

^e Department of Community Ecology, Helmholtz-Centre for Environmental Research – UFZ, Theodor-Lieser-Straße 4, 06120 Halle, Germany

^f Université de Lyon, Université Lyon 1, CNRS, VetAgro Sup, UMR 5558, Laboratoire de Biométrie et Biologie Evolutive, 69622 Villeurbanne, France



GRAPHICAL ABSTRACT



ARTICLE INFO

Editor: R. Sara

Keywords:

Toxicity

Multi-omics

Microalgae

Metabolic pathway

Concentration-response modelling

ABSTRACT

In aquatic ecosystems, the biocide triclosan represents a hazard for the non-target microalgae. So far, algal responses were mainly investigated at apical levels hampering the acquisition of a holistic view on primary, adaptive, and compensatory stress responses. We assessed responses of the chlorophyte *Scenedesmus vacuolatus* to triclosan at apical (growth, photosynthesis) and molecular (transcriptome, metabolome) levels for comparative pathway sensitivity analysis. For each responsive signal (contigs, metabolites), a concentration-response curve was modeled and effect concentrations were calculated leading to the setting of cumulative sensitivity distributions. Molecular responses showed higher sensitivity than apical observations. The functional annotation of contigs and metabolites revealed 118 metabolic pathways putatively impaired by triclosan, highlighting a wide repercussion on the algal metabolism. Metabolites involved in the lipid metabolism showed decreasing trends along the concentration gradient and a globally highest sensitivity, pointing to the primary target of triclosan. The pathways involved in xenobiotic degradation and membrane transporters were mainly regulated in the transcriptome with increasing response trends comprising compensatory responses. The suggested novel approach, combining apical and multi-omics analyses in a concentration-response framework improves mechanistic understanding and mode of action analysis on non-targeted organisms and is suggested to better implement high-throughput multi-omics data in environmental risk assessment.

* Corresponding authors.

E-mail addresses: floriane.larras@ufz.de (F. Larras), mechthild.schmitt@ufz.de (M. Schmitt-Jansen).

<https://doi.org/10.1016/j.jhazmat.2020.122727>

Received 15 January 2020; Received in revised form 28 March 2020; Accepted 11 April 2020

Available online 18 April 2020

0304-3894/ © 2020 The Authors. Published by Elsevier B.V. This is an open access article under the CC BY-NC-ND license

(<http://creativecommons.org/licenses/by-nc-nd/4.0/>).

1. Introduction

The recent rise of omics techniques like genomics, transcriptomics, proteomics and metabolomics has opened new perspectives in the field of risk assessment of environmental stressors (e.g. chemical pollutants). Since decades, the use of apical endpoints including growth, photosynthesis and mortality, has been in the focus of research assessing the sensitivity of organisms to a stressor and to define protective thresholds for biological communities. While apical endpoints are mostly based on a direct measurement of physiological or morphological parameters, omics methods measure responses at the molecular level. That includes different measures such as genomic diversity, transcript, protein and metabolite abundance to investigate e.g. disturbances of metabolic pathways, adaptation and diversification, or evolutionary trajectories. As biological processes at the molecular scale support apical endpoints, omics responses might provide insights into effect propagation across biological scales as well as in modes of actions of chemicals or defense mechanisms. Essentially, effect assessment at the molecular level allows retrieving early responses related to the molecular initiating or early key events induced by a stressor as illustrated by the Adverse-Outcome-Pathway concept (Ankley et al., 2010; Brockmeier et al., 2017). Therefore, these molecular responses could be used to predict effects at apical level or to group chemicals. Several studies have recently highlighted the benefit of omics approaches in ecotoxicology (Beale et al., 2016; Wang et al., 2018; Zhang et al., 2018). More specifically, authors have demonstrated omics techniques to be adequate for discovering herbicide biomarkers (Moisset et al., 2015; Pesce et al., 2013), understanding the mechanisms of interactions between chemicals and organisms (Pillai et al., 2014; Schüttler et al., 2017), and for assessing metabolic responses of micro- or macrophytes (Beauvais-Flück et al., 2016; Dranguet et al., 2017), fish (Sotton et al., 2019) and microbial communities (Beale et al., 2017) to various stressors *in-situ*.

Most omics studies for chemical effects currently rely on the assessment of one 'omics' level (typically transcriptome, metabolome or proteome) at one time point and one concentration. Such approaches can represent a first step towards mechanistic understanding but may not be sufficient as they provide partial information on molecular responses which are dynamic over time and concentration-dependent, and may not propagate linearly across different molecular levels. It was shown that selected 'omics' levels differed regarding the time window of responses in specific pathways. For example, the microalgae *Chlamydomonas reinhardtii* showed different pathway-specific response patterns at different time points following exposure to silver in the transcriptome and the proteome (Pillai et al., 2014). Thus, combining observations obtained at different omics levels may provide a more integrative picture of organisms' responses, supporting *in fine* the mechanistic understanding of chemical effects on biota. Depending on the mode of action, and whether the interaction is primarily at a receptor level (e.g. binding to a transcription factor) or interferes with the biosynthesis of cellular macromolecules (e.g. fatty acid synthesis) the specific 'omics' approach would either reflect the specific interaction or more unspecific secondary responses. Hence, a combination of different 'omics' levels is likely to improve the identification of mode of action related information that may finally be used to understand population responses as part of a risk assessment. Therefore, the scientific community has developed numerous tools that combine omics data (Pinu et al., 2019), mainly designed for integrative pathway investigation but rarely provide outputs usable to derive thresholds or points of departure for chemical effects.

Combining complex responses at different biological levels represents a challenge because different experimental designs are often used for each level (e.g. exposure time, number of replicates), the way they are measured (e.g. different extraction methods, chemical-analytical tools, pre-processing of data) and the nature of the data (e.g. different entities, units). After data acquisition, they are often analyzed in parallel using heatmaps or combined by multivariate analyses (e.g.

canonical analysis) or by applying network analysis. Omics studies consisting of a few exposure concentrations or durations allow detecting up-down regulation, deriving fold change of expression and correlation network analysis. However, molecular items may respond in different, non-linear response characteristics that either reflects interaction with the molecular target or secondary compensatory responses and may additionally depend on toxicokinetics. Therefore, a quantitative concentration-dependent comparison of responses can enable a better mechanistic understanding of molecular stress responses (Schüttler et al., 2019). Furthermore, quantitative information in terms of protective thresholds (i.e. "safe exposure concentrations not exceeding an acceptable impact on biological communities") cannot be concluded by current experimental designs hampering the integration of omics-results in current risk assessment procedures. So far, a concentration-response framework for omics data represents a promising approach towards risk assessment (Gündel et al., 2012; Larras et al., 2018; Schüttler et al., 2019; Smetanová et al., 2015; Thomas et al., 2007; Wang et al., 2018). It could improve the integration of molecular approaches in ecological risk assessment procedures, in a single as well as a multi-omics context. Additionally, this design may allow going further in the interpretation of molecular responses by defining response trends and metrics such as effect thresholds for each specific element, and in this way aligns with the usual methodology of ecological risk assessment. As these metrics represent a common language between molecular level (and apical levels) we assume that quantitative comparison between them can be obtained. To overcome the challenges of modelling concentration-response curves from high-throughput data, a turnkey tool was recently developed (Larras et al., 2018). Here we address a further challenge towards a quantitative comparison of high-throughput omics data by providing a conceptual framework for comparison of response sensitivities on pathway level.

The overall aim of this study was to illustrate the added-value of a system-wide approach in a concentration-response framework to improve mechanistic understanding of toxicants on non-target organisms. In detail our questions were: (i) How can multi-omics and phenotypic data be integrated for quantitative comparison? (ii) Which additional information does this approach provides towards mechanistic understanding in comparison to classical apical endpoints? (iii) Does the approach support the mode of action analysis of a model compound (triclosan) in non-target organisms (chlorophytes) and (iv) enable a better integration of multi-omics data in risk assessment of chemicals in non-target organisms?

To address these questions, synchronized cultures of the chlorophyte *Scenedesmus vacuolatus* were exposed for 14 h to the biocide triclosan in a concentration-response design and analyzed at the transcriptome, the metabolome and at apical levels. This alga is an established ecotoxicological model for the analysis of toxic effects on eukaryotes which can be maintained under synchronous growth of the population. This is of particular relevance for the assessment of molecular responses since all cells are in the same developmental stage. Triclosan, a biocide used in personal care products, is characterized by a specific mode of action in bacteria impairing lipid biosynthesis by inhibiting the enzyme enoyl-acyl carrier protein reductase. Due to this mode of action, this chemical has the potential to impair a wide range of non-target organisms including also microalgae (Eriksson et al., 2015; Machado and Soares, 2019; Pinckney et al., 2017; Tato and Beiras, 2019; Xin et al., 2019). Triclosan has been identified to represent a hazard for algae in water systems (Busch et al., 2016). It has been shown that triclosan induces several effects at the molecular level in microalgae (e.g. increase of superoxide dismutase transcription (Pan et al., 2018)) but so far, the specific mode of action in algae remains unconfirmed. Further, the estimation of protective thresholds was only performed at the apical level (Capdevielle et al., 2008; von der Ohe et al., 2012). In the present study we hypothesize that working in a concentration-response and multi-omics framework enhances mechanistic understanding of triclosan effects in microalgae and provide

specific information on the mode of action. Classically investigated apical endpoints applied in risk assessment (e.g. growth, photosynthesis) are clearer related to ecological processes than molecular endpoints. However, molecular stress responses might have the advantage to provide mechanistic understanding on effect propagation, and hence, contribute to a better informed risk assessment, ultimately enabling extrapolation of effects on the population level in future (Ankley et al., 2010). The interest to investigate both transcriptome and metabolome responses is that they provide complementary information depending on the mode of action of the test compounds. Transcriptomics reveals the expression level of genes, which may represent a primary (e.g. in case of interference with transcription factors) or secondary response (adaptation or stress responses). The metabolome represents a direct signature of biochemical activities (balance between synthesis and degradation of metabolites). Both may be correlated (Bundy et al., 2008; Jamers et al., 2013), but it has to be taken in account that the responses may manifest after different durations of exposure (Jamers et al., 2013; Pillai et al., 2014).

2. Material and methods

2.1. Algal culture

Synchronized cultures of the chlorophyte *Scenedesmus vacuolatus* (Shih. et Krauss strain 211-15, culture collection Pringsheim (SAG Göttingen, Germany)) were grown photoautotrophically in a sterile inorganic medium (pH 6.4) at 28 °C. To keep the cultures in synchronized and exponential growth conditions, a 14:10-h light:dark cycle and a daily dilution to a standard cell density of 10^6 cells mL⁻¹ before the onset of light were chosen. More details on the media and the culture conditions can be found in a previous study (Altenburger et al., 2004).

2.2. Experimental design

For the analysis of the transcriptome, algae were exposed to 5 concentrations ranging from 0.69 to 6.63 µg/L of triclosan (CalbioChem, Germany, purity 99.8 %) while for the metabolome, 6 concentrations ranging from 0.69 to 7.76 µg/L were chosen. For both molecular levels, a solvent-control (DMSO at the concentration of 0.1 %) was included. For the metabolome, a control without solvent was also taken into consideration but no differences were found between the algal metabolome of control without and control with DMSO. Stability of triclosan in the medium was tested for two exposure concentrations (N = 9 each) during the experiment by liquid chromatography-high resolution mass spectrometry (LC-HRMS) using a Ultimate 3000 LC coupled to a LTQ Orbitrap XL mass spectrometer (Thermo). A recovery rate of 81 % and 87 % was obtained, respectively. In both cases, the exposure lasted 14 h (full light phase of synchronised growth). This duration of exposure is related to the culture synchronization cycle. This allowed to work on a large population of actively growing algal cells. We considered the algal growth phase as a relevant process in this study, since growth is accompanied with an on-going metabolic activity.

For the transcriptome, 5 replicates were used for each concentration. For the metabolome, the controls were replicated 6 times and 2–3 replicates were used for each triclosan exposure concentration. Exposures were performed in 500 mL flasks containing 10^6 cells per mL. Photosynthesis and growth responses were assessed along a concentration gradient of 9 concentrations ranging from 0.1–70.7 µg/L in order to better fit with the reported response of microalgae to triclosan (Franz et al., 2008).

2.3. Metabolome analysis

Briefly, 15 µL of fresh biomass (30 mL suspension in the case of the unexposed algae) were harvested after 14 h of growth by centrifugation

(22 °C, 2 min, 4000 × g). Metabolites were extracted using a solvent mixture of methanol, chloroform and 0.015 % trifluoroacetic acid in water (10:5:4, v/v/v) with ribitol (10 mg/L) as an internal standard. Cells were disrupted using a FastPrep24 homogenizer (MP Biomedicals, Eschwege, Germany). Subsequently, the homogenates were centrifuged (6 min, 6 °C, 20,000 × g) and 1 mL of the supernatant was transferred into a 10 mL glass tube. Hydrophilic and lipophilic metabolites were separated by adding 0.8 mL bi-distilled water and 1.6 mL chloroform followed by intense shaking and centrifugation. After phase separation, 1 mL from the upper hydrophilic methanol/water phase and 1.3 mL from the lower lipophilic chloroform/methanol phase were transferred into 3 mL reaction glass vials. Samples were dried at 40 °C under a nitrogen stream for a maximum of 3 h. Compounds from hydrophilic extracts were methoximated using 200 µL MOXsolution for 120 min at 80 °C. Compounds from the lipophilic extracts were esterified with 300 µL methanolic HCl for 240 min at 80 °C. Afterwards, both fractions were dried under a stream of nitrogen at 40 °C and silylated in 100 µL of MSTFA for 20 min at 90 °C. Metabolites were analyzed using an Agilent 6890 N gas chromatograph coupled to a quadrupole 5975 mass spectrometric detector (GC/MS) guided by the Agilent ChemStation software (G1712DA, Rev. 02.00). From GC/MS analysis, peaks were deconvoluted and identified by using AMDIS with a matching to the mass spectra (match factor > 90 %) against an inhouse library, NIST database, Golm Metabolome Database and Fiehn library.

Area Under the Curve (AuC) - values were obtained for 224 metabolites. Then, we applied the following procedure: i) removing of metabolites for which the proportion of missing data (no detections) across all the samples is higher than 50 percent, ii) retrieving of missing values data using half minimum method (i.e. half of the minimum value found for a metabolite across all samples), iii) log₁₀-transformation of AuC-values.

2.4. RNA extraction and microarray analysis

Algal cultures were harvested by centrifugation (22 °C, 10 min, 3300 × g), and total RNA was extracted based on a combination of TRIzol® (Thermo Fisher Scientific, USA) and mechanical cell lysis using a FastPrep24 homogenizer (MP Biomedicals, Eschwege, Germany). Total RNA was further purified using a RNeasy Plant Mini Kit (Qiagen, Hilden, Germany) according to manufacturer's instructions. Transcriptome responses were assessed using a 8 × 60 L microarray specific for *S. vacuolatus*, and designed with eArray (Agilent Technologies, Böblingen Germany) as already explained (Larras et al., 2018). Each array consists of 61535 probes representing 21495 contigs. For labeling, 50 ng purified RNA was labeled using the Low Input Quick Amp Labeling Kit, one color (Agilent Technologies), and 40 µL of cy3-labeled fragmented cRNA per sample were hybridized to the microarrays for 17 h at 65 °C. The microarrays were washed and scanned, using an Agilent DNA Microarray scanner, and fluorescence intensities were evaluated using the Agilent Feature Extraction software. Genome information (cDNA sequences) have been deposited in NCBI's Sequence Read Archive and are accessible through the SRA accession number PRJNA498405 (<https://www.ncbi.nlm.nih.gov/sra/PRJNA498405>). The fluorescence data have been deposited in NCBI's Gene Expression Omnibus and are accessible via GEO Series accession number GSE122159 (<https://www.ncbi.nlm.nih.gov/geo/query/acc.cgi?acc=GSE122159>).

Fluorescence raw data were finally log₂ transformed.

2.5. Measurement of apical endpoints

Cell volume growth was estimated by a cell particle counter (CASY II, Schärfe System, Reutlingen, Germany) as described by Altenburger et al. (2004). Effects on photosynthesis were quantified by measuring the maximum quantum yield of the photosystem II with the saturation-pulse method by using a MAXI-imaging PAM-fluorometer (HeinzWalz

GmbH, Effeltrich, Germany) after 14 h of exposure. Inhibition of photosynthesis was calculated as relative inhibition of the maximum quantum yield of the photosystem II (Fv/Fm) in comparison to untreated controls; more details on the measuring device and related settings are given in Franz et al. (2008).

2.6. Processing of apical and molecular responses

2.6.1. Metabolome and transcriptome dataset

Our aim at this working step was 1) to identify the responsive elements of the transcriptome (= probes or gene transcripts) and the metabolome (=metabolites) to triclosan, 2) to derive their response trends (e.g. increase, decrease, U-shape, bell-shape) along the concentration gradient and 3) to calculate their effect concentrations as benchmark dose (BMD) based on modelled response curves.

Both, the transcriptomics and metabolomics datasets were analysed by the DRomics tool (Larras et al., 2018), designed to handle 'omics' datasets obtained in a concentration-response framework (Fig. 1). Data were analysed using the DRomics R package version 2.0-1 (Delignette-Muller et al., 2019). In the first step (import and pre-treatment), the transcriptome dataset was normalized between arrays using the cyclic loess method. In the second step (selection of responsive items), the probes and the metabolites which displayed a significant change of the signal along the concentration gradient were identified using a quadratic trend test with a False Discovery Rate (Benjamini-Hochberg test) of 0.01 for the transcriptome and 0.1 for the metabolome. Third, concentration-response modelling was conducted for each of the selected probes and metabolites based on the nominal concentrations. All of the dose-response curves built for each probe and metabolite are presented in Tables A1 and A2, respectively. Fourth, the model with the best fit was used to derive a benchmark dose (BMD-1SD) according to EFSA guidance (EFSA Scientific Committee et al., 2017). This BMD-1SD does not refer to a specific level of effect but indicates the concentration leading to a level of change compared to the control response that takes data variability around the modelled curve into account. It is calculated as the concentration corresponding to a Benchmark Response (BMR-zSD) defined as follows: $BMR-zSD = y_0 + /- z * SD$, where y_0 is the mean control response, and SD is the residual standard deviation of the considered concentration-response model and z is the factor of SD (z fixed at 1 by default). DRomics versions > 2.0 include the calculation of confidence intervals around the BMD value using a bootstrap procedure (Delignette-Muller et al., 2019).

The DRomics tool identified 6361 responsive probes and 68 responsive metabolites and computed for each of them a BMD value and corresponding 95 % confidence intervals. In several cases, the microarray design included for a same contig (assumed to represent one gene) the duplication of a same probe and/or the presence of two different probes. For each contig, we thus had results from 1 to 4 probes. For downstream analysis, only one probe was kept per contig (n = 3177). This probe was the one presenting the narrowest confidence interval around the BMD.

2.6.2. Growth and photosynthesis responses

For each of the two apical endpoints, a concentration-response curve was built (Hill model fitted by non-linear regression) and a BMD-1SD value was derived following the same methodology as in the DRomics tool.

2.7. Functional analysis

Because the main interest of this study was to work on concentration-dependent contigs, only the sequences of the 3177 contigs remaining after the DRomics analysis were blasted against the NCBI nr database (used on the 15th July 2019, taxa investigated: chlorophytes, cyanobacteria, diatoms and Arabidopsis; e-value = 0.001) using the DIAMOND tool (Buchfink et al., 2015). A NCBI code was obtained for

1612 contigs. Enzyme number was retrieved for 507 contigs via the UNIPROT tool (The UniProt Consortium, 2019). A Kyoto Encyclopedia of Genes and Genomes (KEGG) (Kanehisa, 2000) code was also retrieved but 443 contigs were finally associated to KEGG pathways relevant for microalgae. Annotation of the 68 metabolites selected by DRomics was performed manually against the KEGG database and 31 metabolites were found with annotations. In this paper, for both transcriptome and metabolome data two main KEGG annotation levels are considered: the pathway class (e.g. lipid metabolism) and the pathway level which represents all of the pathways belonging to a pathway class (e.g. fatty acid metabolism, energy metabolism).

3. Results

3.1. Response characterization of transcriptomic, metabolic and apical endpoints

The responses of the 3177 contigs and 68 metabolites along the increasing concentration gradient of triclosan were classified in 4 main trends (increase, decrease, bell-shape, U-shape) (Table 1). The metabolome and the transcriptome displayed contrasting trend patterns (statistically significant according to a Chi-square test, p-value < 10^{-5}). While in the transcriptome 34 % of contigs we characterized by increasing trends, the majority of metabolites (54 %) followed decreasing trends. Non-monotonic responses at metabolome and

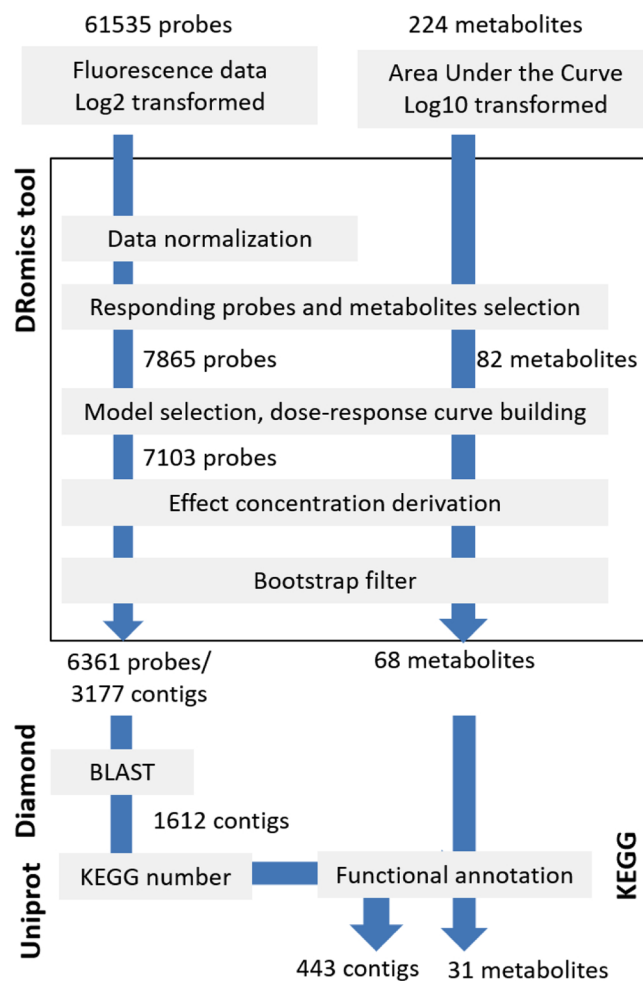


Fig. 1. Overview of the workflow aiming extracting responsive metabolites and contigs after exposure of *S. vacuolatus* to triclosan; For each item, response trends, BMD values and functional KEGG annotations are derived. Numbers indicate the remaining contigs and metabolites after each step.

transcriptome levels accounted for 33 % and 38 %, respectively. Growth exhibited an increasing sigmoid signal of inhibition along the concentration gradient while photosynthesis exhibited hormesis at the lowest concentration (Fig. A1). We modeled the response with a Hill model to omit the hormesis and capture only the inhibition phase.

For each molecular level, a cumulative sensitivity distribution (CSD) of effects concentrations (here, BMD-1SD) was built on 1/ all annotated metabolites or contigs, and 2/ all non-annotated metabolites or contigs (Fig. 2). For both molecular levels, a major proportion of items were not annotated according to the KEGG database (54.4 and 84 %, respectively), however, non-annotated metabolites and contigs exhibited BMD-1SD frequency distributions comparable to those of the annotated ones. Effect concentrations from metabolites (here, BMD-1SD values) for triclosan exposure were found in a wide range of exposure concentration, from 0.11 to 7 $\mu\text{g/L}$. The effect concentrations for transcript abundance showed a comparable range from 0.02–6.1 $\mu\text{g/L}$. Non-annotated metabolites and contigs exhibited BMD-1SD frequency distributions comparable to those of the annotated ones. Growth and photosynthesis displayed BMD-1SD values of 11.8 and 28.6 $\mu\text{g/L}$, respectively (Fig. A1). The maximum tested concentrations led to 77 % and 29 % of growth and photosynthesis inhibition, respectively.

3.2. Metabolic pathway responses

The results presented in the following part are exclusively based on the 443 contigs and the 31 metabolites which were KEGG-annotated.

3.2.1. Impaired metabolic pathways

Fig. 3 illustrates the total number of metabolites and contigs associated to each pathway class. The number of molecular items was highly variable between classes and ranged from 6 (biosynthesis of other secondary metabolites) to 88 (carbohydrate metabolism). Based on both molecular levels, 18 classes of pathways were impaired by triclosan after 14 h of exposure (17 according to transcriptome, 9 according to metabolome). Eight classes of pathways which were mainly related to metabolism (e.g. carbohydrate, amino acid, lipid and energy metabolism), were impaired at both molecular levels. Most contigs were mainly associated to one pathway class, but numerous metabolites were associated to more than one (Fig. A2). As each class of pathway is composed of several underlying pathways, we noticed that overall, 118 underlying pathways were potentially impaired. Lipid metabolism is the pathway class exhibiting the highest number of underlying pathways for which at least one metabolite or contig was impaired by triclosan (Table A3) (15 among which biosynthesis of unsaturated fatty acids and fatty acid biosynthesis), followed by the carbohydrate metabolism and the amino acid metabolism (14 each). In all pathway classes a high coverage of underlying pathways was found according to the KEGG-classification (e.g. 15 out of 17 underlying pathways for lipid metabolism, 14 out of 15 for carbohydrate metabolism).

3.2.2. Response trends, signal intensity and sensitivity of pathway classes

For each of the 18 pathway classes, a CSD was set at the transcriptome level (resp. metabolome) using the BMD-1SD value of all contigs (resp. metabolites) implied in this pathway class. Nine CSDs could be created based on metabolites and 17 CSDs based on contigs. For some pathway classes responses were only found in the transcriptome (e.g. xenobiotics biodegradation or transport and catabolism). Each distribution displayed the response of each contig or metabolite involved in this pathway class (see Fig. 4 for the example of lipid metabolism and Figs. A3 and A4 for the other pathways) in terms of i) trend (represented by the dot shape) and ii) signal intensity (represented by color gradient) based on fluorescence in log2 for transcriptome and AUC in log10 for metabolome, centered by the signal of the control for each item and iii) sensitivity towards triclosan exposure (BMD-1SD value). A heat map analysis was not considered since it does not easily allow to capture the differential sensitivity of genes and

pathways. In contrast, calculation of BMDs and derivation of CSDs represent a direct quantitative assessment of the sensitivity of genes and pathways and is therefore more appropriate.

- i) As a general finding, pathways could not exclusively be related to a main response trend, rather a high variability of response trends was observed within a molecular level for a same pathway class; nevertheless, differences between pathway response trends became obvious. The metabolites involved in lipid metabolism did not show any increasing trend, but a clear dominance of decreasing trends (75 %, concentration-response curves are shown in Fig. A5), while the other pathways showed a dominance of non-monotonic trends in the metabolome. In comparison, the most sensitive contigs associated to lipid metabolism were mostly U-shaped (concentration-response curves are shown in Fig. A6).
- ii) Regarding the signal intensity, the transcriptome displayed a stronger signal variation than the metabolome. For example, if inhibition of metabolome and transcriptome expressions in terms of fold change are similar (see lower level of the signal range Fig. 4, $10^{-0.8} = 0.16$ and $2^{-2.5} = 0.18$ respectively), transcriptome displayed higher overexpression level (see upper level of the signal range Fig. 4, fold change up to $2^{7.5} = 181$) than metabolome (up to $10^{0.8} = 6.3$), but for a few items only, as the one clearly appearing in Fig. A4 for “folding, sorting and degradation” pathway.
- iii) To be able to compare the sensitivity of affected pathways to triclosan, we derived the 25th percentile of the CSD specific to each class of pathway and for each molecular level (from data presented Figs. 4 and A3–A4). The 25th percentile represents a concentration where 25 % of contigs or metabolites involved in a specific pathway were affected (according to their BMD levels). A level of 25 % was selected because of the statistical limitations due to low numbers of items per pathway class to derive robust lower percentile values. These thresholds ranged, depending on the pathway class, from 0.72 to 1.99 $\mu\text{g/L}$ for the transcriptome and from 0.23 to 1.39 $\mu\text{g/L}$ for the metabolome (Fig. 5). Depending on the molecular level, the pathway classes exhibited different sensitivities, however all thresholds remained finally in a small range of concentrations. The most sensitive pathway class was the lipid metabolism; additionally, it showed one of the biggest contrasts in thresholds between the metabolome and the transcriptome (0.23 and 1.12 $\mu\text{g/L}$, respectively). The most sensitive metabolites were mostly associated to the underlying pathways of biosynthesis of unsaturated fatty acids, alpha-linoleic acid metabolism and linoleic and glycerophospholipid metabolism. Transcriptional regulation of membrane transport was the second most sensitive pathway with the underlying pathway of ABC transporters regulated. Several pathways, related to detoxification were mainly regulated in the transcriptome (e.g. xenobiotic biodegradation). Contigs associated to proteins known to deal with detoxification processes and more specifically oxidative stress defense mechanisms (ascorbate peroxidase (= “carbohydrate metabolism” and “metabolism of other amino acids”), catalase (= “carbohydrate metabolism” and “amino acid metabolism”), thioredoxin (= “metabolism of other amino acids”), Glutathione S-transferase (= “metabolism of other amino acids” and “xenobiotic degradation and metabolism)) exhibited

Table 1

Number of metabolites and contigs (and percentage into brackets) associated to each of the four response trends. A Chi-square test indicates that the trend distributions are different in metabolites and contigs ($p < 10^{-5}$).

Trend	Metabolites	Contigs
Increase	9 (13 %)	1092 (34 %)
Decrease	37 (54 %)	878 (28 %)
Bell	12 (18 %)	546 (17 %)
U	10 (15 %)	661 (21 %)

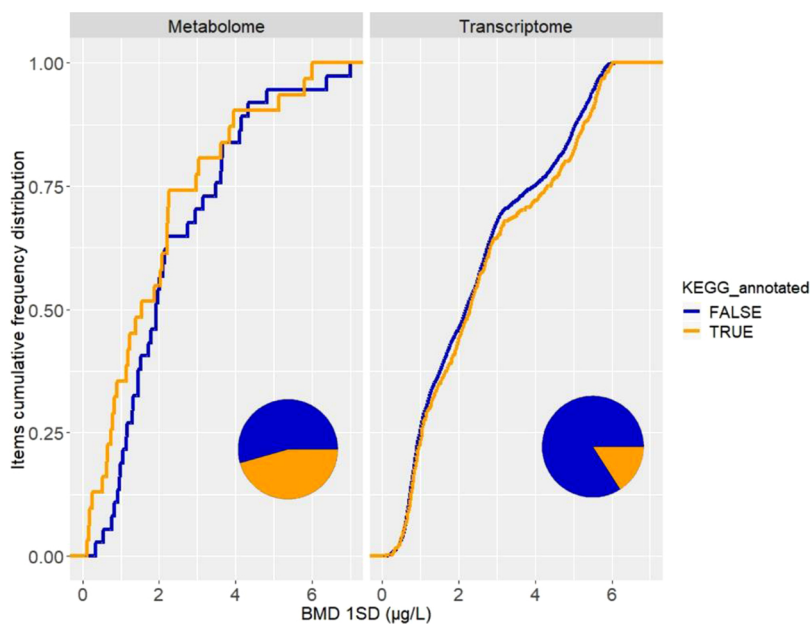


Fig. 2. Cumulative distributions of the BMD values for the metabolome and the transcriptome for non-annotated (blue) and annotated (orange) items. Pie charts represent the proportion of annotated and non-annotated metabolites and contigs identified as responsive to triclosan. The BMD-1SD is the concentration corresponding to a Benchmark Response (BMR-zSD) defined as follows: $BMR-zSD = y_0 + / - z * SD$, where y_0 is the mean control response, and SD is the residual standard deviation of the considered concentration-response model and z is the factor of SD (z fixed at 1 by default).

mostly an increasing expression trend towards the highest concentrations (concentration-response curves are shown in Fig. A7).

4. Discussion

The management and interpretation of stress responses at different molecular levels represents an issue faced by multiple research areas (e.g. food risk, medicine, ecological risk). This is demonstrated by the recent rising of works providing recommendations as how to better

support multi-omics studies (Beale et al., 2016; Haas et al., 2017; Misra et al., 2019; Pinu et al., 2019). In our study, we used the power of the concentration-response framework which allowed us the combination of multi-omics levels and enabled a quantitative comparison of dynamic molecular responses in cumulative sensitivity distributions. We especially paid attention to manage the data of those two molecular levels regarding their nature and the way they were obtained. The transcriptome and the metabolome datasets were both analyzed by the same statistical workflow (Fig. 1) using the DRomics tool (Larras et al.,

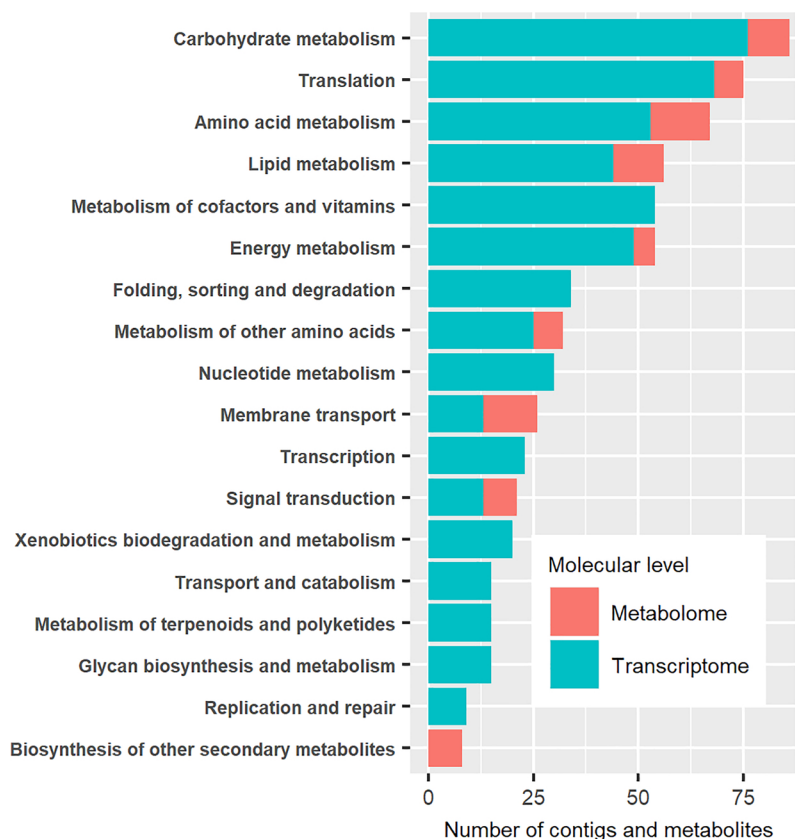


Fig. 3. Number of responsive contigs and metabolites per KEGG pathway class.

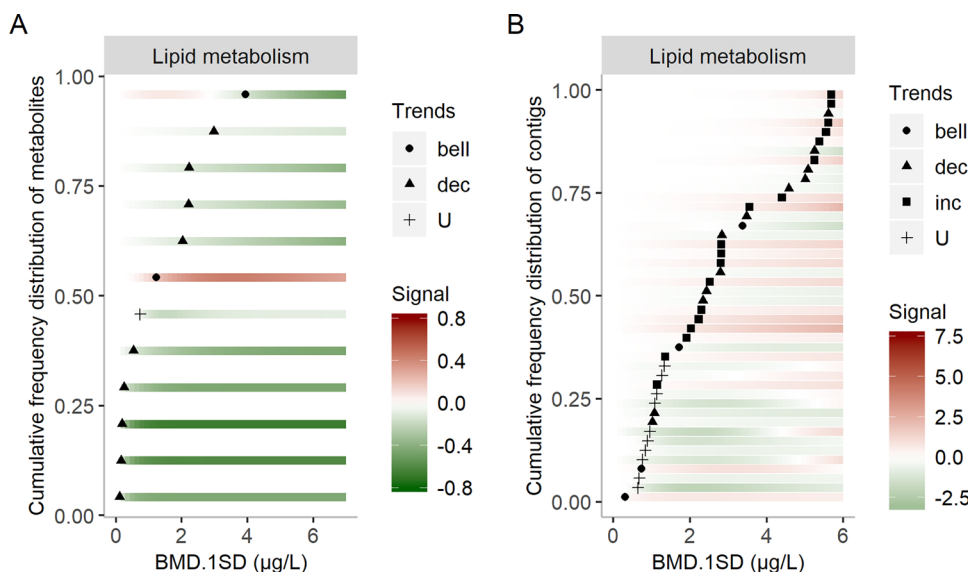


Fig. 4. Cumulative sensitivity distribution (CSDs) of (A) metabolites and (B) contigs. As an example CSDs involved in lipid metabolism based on their BMD-1SDs are shown. Item response trend is represented by the shape (circle = bell shaped, diamond = decreasing, square = increasing and cross = u-shaped trend) and item signal intensity response along the concentration gradient is represented by the color gradient (from green = inhibition compared to control, to red = over-expression compared to control). CSDs for other pathways are depicted in Figs. A3 and A4. The BMD-1SD is the concentration corresponding to a Benchmark Response (BMR-zSD) defined as follows: $BMR-zSD = y_0 + /- z \cdot SD$, where y_0 is the mean control response, and SD is the residual standard deviation of the considered concentration-response model and z is the factor of SD (z fixed at 1 by default).

2018). Thus, we considered the metrics related to the concentration-response approach (e.g. BMD, response trend) as a common language between those levels allowing interpreting and managing data in a comparable way. So far, such approaches have been realized only on one molecular level (Gündel et al., 2012; Wang et al., 2018), or on different molecular levels but from distinct species and without sensitivity thresholds derivation (Smetanová et al., 2015).

4.1. Complexity of molecular responses

Metabolite and contigs responses to triclosan exposure showed a remarkable complexity in terms of variety of (i) response trends, (ii) signal intensities and (iii) sensitivities. This response diversity was found at both molecular levels as well as within individual pathways. From the initial set of metabolites (n = 224) and contigs (n = 21495) measured in this study, 30 % of each were significantly impaired by the biocide. Also, almost all pathway classes of the basic metabolism (according to the KEGG-database) of the chlorophyte were disturbed with a high coverage of the underlying pathways, indicating severe and

unspecific impacts on the global metabolism of the chlorophyte or even compensatory responses. To disentangle these complex response patterns, new approaches (e.g. a combination of omics responses or the development of tools that enable the management of different omics levels in a comparable way to obtain a more integrative response picture) were needed to improve our mechanistic understanding of stress responses and to be able to make use of gained information (e.g. mode of action analysis and ERA).

4.2. Comparative assessment of transcriptome and metabolome

Principally, a multi-omics approach may allow capturing a wider variety of mechanisms with increased specificity, given that depending on the primary target, specific responses may show differential sensitivity compared to unspecific and compensatory responses. Therefore, affected pathways were ranked in CSDs. We partly found contrasting patterns between both molecular levels with some changes apparent only for one molecular level (e.g. xenobiotic biodegradation or metabolism of co-factors and metabolites). This might indicate cellular

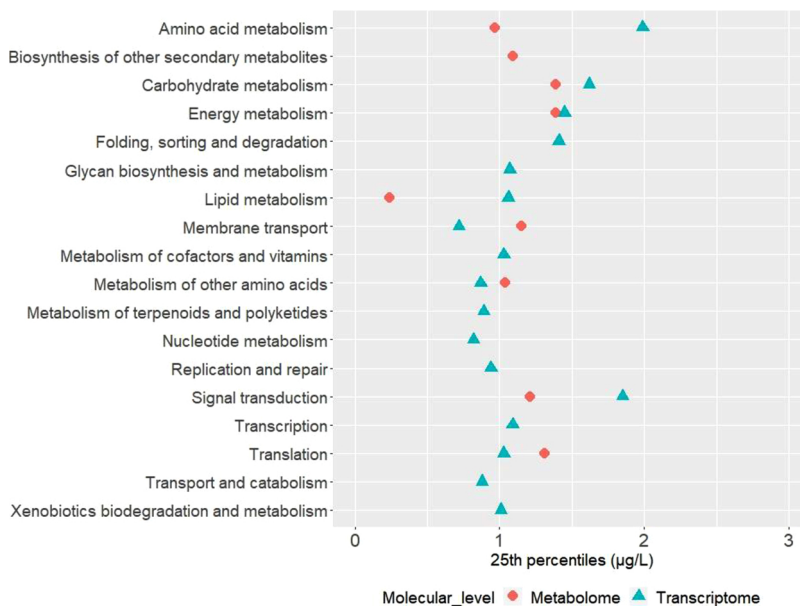


Fig. 5. Sensitivity of pathway classes (according to KEGG-classification) based on the 25th percentile of BMD values related to contigs (green diamond) and metabolites (red circle).

regulation processes in the transcriptome at the investigated time point (14 h of exposure) which have not been detected at the metabolome level (because of time-response delay or because such pathways are not responsive at this level). Contrasting patterns were also found in terms of sensitivity. The higher sensitivity of metabolomics in comparison to transcriptomics in the lipid metabolism hints to the primary target of the toxicant. Our results indicate the added value of a multi-omics approach aiming to understand regulation processes and to define effect thresholds. Pillai et al. (2014) also observed that the transcriptome and the proteome of the microalgae *Chlamydomonas reinhardtii* exposed to silver did not always reconstitute the same information in terms of impaired metabolic pathways and expression changes. Such results may be due to the different time needed by each level to respond (Haider and Pal, 2013; Pillai et al., 2014) or because one level is more closely related to the primary molecular target than another.

4.3. Concentration response analysis

A strong variety of response trends was observed at both molecular levels. More than one third of the data was characterized by a non-monotonic response and rarely matched with the Hill model commonly used in ecotoxicology, indicating regulation processes on pathway level rather than the inhibition of metabolic activities. Such a variety in response trends was also reported for the zebrafish embryo transcriptome (Smetanová et al., 2015; Wang et al., 2018), proteome (Gündel et al., 2012) and the macrophyte *Myriophyllum spicatum* metabolome (Riedl et al., 2015) and may be associated with different functions in the metabolism. For example, most sensitive contigs associated to the lipid metabolism exhibited a U-shape response across the concentration gradient suggesting regulation to compensate an inhibition at higher concentrations. Conversely, Bell-shaped curves may show a point of disruption where metabolism cannot cope anymore with the stress. If such trends constituted more than one third of the responses observed per molecular level, the diversity of responses obtained per pathway (due to the numerous items include in each of them) prevents to highlight clear compensation trends for specific metabolic pathways. Such trends may nevertheless become evident for individual items and pathways.

Of course, those results are specific to the exposure time, which is always a tricky choice standing at the interface between the biological characteristics of the organism and the aim of the study. Our opinion is that a short exposure time (e.g. 15 min (Pillai et al., 2014); 2 h (Beauvais-Flück et al., 2016)) is needed to differentiate between primary and secondary effects using the suggested approach. However, a more complete picture including the assessment of the dynamic regulation of stress responses, may benefit from extended exposures but would require a combined concentration – time response analysis.

4.4. Inferring mode of action information from pathway-specific analysis

Triclosan is known to inhibit the activity of the *FabI* gene encoded enzyme enoyl-acyl carrier protein reductase in bacteria (McMurry et al., 1998) which is the last enzyme in the fatty acid elongation cycle. Thus, we assumed that the lipid metabolism of *S. vacuolatus* may be specifically impaired. This assumption was firstly supported by the 25th percentile threshold obtained for the lipid metabolism at the metabolome level, the highest sensitivity among all affected biochemical pathways. Second, the dose-response approach highlighted that among all of the impaired pathways, most of the metabolites associated to lipid metabolism showed a monotonically decreasing trend along the concentration gradient. Of the biochemical pathways, this trend was only found for lipid metabolism, which indicates that the underlying pathways (e.g. biosynthesis of unsaturated fatty acids, alpha-linolenic metabolism) could not be compensated by other pathways. This result essentially points to the mode of action of triclosan in *S. vacuolatus*. A recent study confirmed that triclosan impaired lipids or fatty acids

related functional groups through quantitative assessment and thus for different microalgae and at concentrations similar to the one used in our study (Xin et al., 2019). Conversely, most sensitive contigs associated to the lipid metabolism displayed a lower sensitivity compared to the metabolome suggesting regulation at higher concentrations. Based on the role of the lipid metabolism in cell growth processes, we also assume that triclosan may have a widespread effect on membrane integrity that at higher dose jeopardizes population growth, which became obvious in the phenotypic observations. In conclusion, the information provided at both molecular levels in terms of trend response and sensitivity supports mode of action characterization of the biocide in this non-target species and confirms the importance of combining responses from different molecular levels when the mode of action of a compound is not fully characterized. Triclosan is further known to induce various responses in a wide diversity of organisms (Alfihli and Lee, 2019; Dhillon et al., 2015). For example, the bacterium *Mycobacterium tuberculosis* exhibited numerous impaired pathways (e.g. lipid metabolism, cell wall), indicated by transcriptome analysis after 6 h of exposure to 8 mg/L of triclosan (Betts et al., 2003). In our study, we observed that triclosan in *S. vacuolatus* induced expression changes at lower concentrations than for bacteria (Betts et al., 2003) and in numerous metabolic pathways at both metabolome and transcriptome levels. Effects on the carbohydrate metabolism and the energy metabolism including photosynthesis at both molecular levels suggest a global secondary effect of triclosan regarding the energy acquisition to compensate for toxic effects. Further, the increasing expression of contigs associated to enzymes involved in detoxification processes (ascorbate peroxidase, catalase, thioredoxin and glutathione s-transferase) revealed that algal cells trigger compensation of reactive oxygen species production and detoxification processes in a dose-dependent way. Those enzymes are especially known to be involved in plant defense mechanisms against oxidative stress (Caverzan et al., 2012; Pillai et al., 2014; Sarkar et al., 2005) and suggest that the cells are able to cope with oxidative stress at least up to 7 µg/L of triclosan.

Effects of other toxic compounds may result in different ranking of sensitivities of molecular levels as well as pathways in dependence of the mode of action and primary target. This illustrates the added value of multi-omics approaches to derive an integrated picture of the toxic response. These conclusions could be drawn despite a low annotation rate at both molecular levels. On the other hand, the comparable results in terms of cumulative sensitivity distributions of the overall metabolic and transcriptomic responses of annotated and non-annotated items, respectively shows the power of this approach and also motivates to make use of the complete untargeted response pattern beyond specific information on the responding items.

4.5. Deriving protective threshold from molecular data

Most studies dealing with effect assessment of triclosan to microalgae have reported effects at the apical levels for single-species experiments in laboratories (Machado and Soares, 2019) as well as for environmental communities (Eriksson et al., 2015; Pinckney et al., 2017) based on apical responses (e.g. growth, photosynthesis). As sensitivity values are mostly related to a higher level of effect (e.g. EC50, Effect Concentration that inhibits 50 % of the biological parameter) and/or higher exposure concentration ranges, the comparison to the values obtained for apical endpoints in our study is restricted. For example, microalgal single-species bioassays have provided various sensitivity values such as 1.4 and 4.7 µg/L (EC50 (von der Ohe et al., 2012)) or 0.5 µg/L (No Observed Effect Concentration (Singer et al., 2002)). Also, most studies exposed for longer exposure times such as 72 h or 96 h (Machado and Soares, 2019; Pinckney et al., 2017) to cover chronic effects, while we worked with a synchronized culture, which provides a 8-fold increase of the population density within 24 h. An exposure of 14 h during the growth phase as performed in this study, is probably beyond acute exposure and a propagation to chronic effects is

reliable based on a time series analyses performed with the same experimental settings (Vogs and Altenburger, 2016). From such values, some of those studies have derived protective thresholds using arbitrary safety factors. To compensate for uncertainty in current risk assessment approaches, safety factors of several orders of magnitude were applied, resulting in Predicted No Effect Concentrations (PNEC) ranging from 1.4 ng/L and 1.6 µg/L (Capdevielle et al., 2008; von der Ohe et al., 2012). However, the choices of these factors are rarely based on scientific rationales. The lowest sensitivity values observed in our study fall in the range of PNEC-values reported in literature indicating that molecular approaches may support current risk assessment approaches by providing more informed protection thresholds based on mechanistic understanding.

CRedit authorship contribution statement

Floriane Larras: Formal analysis, Visualization, Writing - original draft. **Elise Billoir:** Software, Investigation, Visualization, Writing - review & editing. **Stefan Scholz:** Conceptualization, Investigation, Writing - review & editing. **Milka Tarkka:** Methodology, Resources. **Tesfaye Wubet:** Methodology, Resources. **Marie-Laure Delignette-Muller:** Software, Formal analysis, Writing - review & editing. **Mechthild Schmitt-Jansen:** Conceptualization, Investigation, Writing - original draft, Supervision.

Declaration of Competing Interest

The authors declare that they have no known Competing financial interests or personal relationships that could have appeared to influence the work reported in this paper.

Acknowledgments

We thank the European Commission for the financial support (MicroERA project, H2020-MSCA-IF-2015 (Grant number: 705149)). This work has been also financially supported by the “Ecosphère continentale et côtière” (EC2CO) interdisciplinary program from the Centre National de la Recherche Scientifique (CNRS, France), as a part of the DROMADERE project. We additionally thank Janet Krüger and Nicole Schweiger for support in the laboratory.

Appendix A. Supplementary data

Supplementary material related to this article can be found, in the online version, at doi:<https://doi.org/10.1016/j.jhazmat.2020.122727>.

References

Alfahli, M.A., Lee, M.-H., 2019. Triclosan: an update on biochemical and molecular mechanisms. *Oxid. Med. Cell. Longev.* 2019, 1–28. <https://doi.org/10.1155/2019/1607304>.

Altenburger, R., Walter, H., Grote, M., 2004. What contributes to the combined effect of a complex mixture? *Environ. Sci. Technol.* 38, 6353–6362. <https://doi.org/10.1021/es049528k>.

Ankley, G.T., Bennett, R.S., Erickson, R.J., Hoff, D.J., Hornung, M.W., Johnson, R.D., Mount, D.R., Nichols, J.W., Russom, C.L., Schmieder, P.K., Serrano, J.A., Tietge, J.E., Villeneuve, D.L., 2010. Adverse outcome pathways: a conceptual framework to support ecotoxicology research and risk assessment. *Environ. Toxicol. Chem.* 29, 730–741. <https://doi.org/10.1002/etc.34>.

Beale, D.J., Karpe, A.V., Ahmed, W., 2016. Beyond metabolomics: a review of multi-omics-based approaches. In: Beale, D.J., Kouremenos, K.A., Palombo, E.A. (Eds.), *Microbial Metabolomics*. Springer International Publishing, Cham, pp. 289–312. https://doi.org/10.1007/978-3-319-46326-1_10.

Beale, D., Karpe, A., Ahmed, W., Cook, S., Morrison, P., Staley, C., Sadowsky, M., Palombo, E., 2017. A community multi-omics approach towards the assessment of surface water quality in an urban river system. *Int. J. Environ. Res. Public Health* 14, 303. <https://doi.org/10.3390/ijerph14030303>.

Beauvais-Flück, R., Slaveykova, V.I., Cosio, C., 2016. Transcriptomic and physiological responses of the green microalga *Chlamydomonas reinhardtii* during short-term exposure to subnanomolar methylmercury concentrations. *Environ. Sci. Technol.* 50, 7126–7134. <https://doi.org/10.1021/acs.est.6b00403>.

Betts, J.C., McLaren, A., Lennon, M.G., Kelly, F.M., Lukey, P.T., Blakemore, S.J., Duncan, K., 2003. Signature gene expression profiles discriminate between isoniazid-, thio-lactomycin-, and triclosan-treated *Mycobacterium tuberculosis*. *Antimicrob. Agents Chemother.* 47, 2903–2913. <https://doi.org/10.1128/AAC.47.9.2903-2913.2003>.

Brockmeier, E.K., Hodges, G., Hutchinson, T.H., Butler, E., Hecker, J., Tolleson, K.E., Garcia-Reyero, N., Kille, P., Becker, D., Chipman, K., Colbourne, J., Collette, T.W., Cossins, A., Cronin, M., Graystock, P., Gutsell, S., Knapen, D., Katsiadaki, I., Lange, A., Marshall, S., Owen, S.F., Perkins, E.J., Plaistow, S., Schroeder, A., Taylor, D., Viant, M., Ankley, G., Falciani, F., 2017. The role of omics in the application of adverse outcome pathways for chemical risk assessment. *Toxicol. Sci.* 158, 252–262. <https://doi.org/10.1093/toxsci/kfx097>.

Buchfink, B., Xie, C., Huson, D.H., 2015. Fast and sensitive protein alignment using DIAMOND. *Nat. Methods* 12, 59–60. <https://doi.org/10.1126/nmeth.3176>.

Bundy, J.G., Sidhu, J.K., Rana, F., Spurgeon, D.J., Svendsen, C., Wren, J.F., Stürzenbaum, S.R., Morgan, A.J., Kille, P., 2008. “Systems toxicology” approach identifies co-ordinated metabolic responses to copper in a terrestrial non-model invertebrate, the earthworm *Lumbricus rubellus*. *BMC Biol.* 6, 25. <https://doi.org/10.1186/1741-7007-6-25>.

Busch, W., Schmidt, S., Kühne, R., Schulze, T., Krauss, M., Altenburger, R., 2016. Micropollutants in European rivers: a mode of action survey to support the development of effect-based tools for water monitoring: micropollutants in European rivers: a mode-of-action. *Environ. Toxicol. Chem.* 35, 1887–1899. <https://doi.org/10.1002/etc.3460>.

Capdevielle, M., Van Egmond, R., Whelan, M., Versteeg, D., Hofmann-Kamensky, M., Inauen, J., Cunningham, V., Woltering, D., 2008. Consideration of exposure and species sensitivity of triclosan in the freshwater environment. *Integr. Environ. Assess. Manag.* 4, 15. <https://doi.org/10.1897/IEAM.2007-022.1>.

Caverzan, A., Passaia, G., Rosa, S.B., Ribeiro, C.W., Lazzarotto, F., Margis-Pinheiro, M., 2012. Plant responses to stresses: role of ascorbate peroxidase in the antioxidant protection. *Genet. Mol. Biol.* 35, 1011–1019. <https://doi.org/10.1590/S1415-47572012000600016>.

Delignette-Muller, M.L., Billoir, E., Larras, F., Siberchicot, A., 2019. DRomics: Dose Response for Omics. Reference Manual. R Package Version 2.0 (Accessed 2nd October 2019).

Dhillon, G., Kaur, S., Pulicharla, R., Brar, S., Cledón, M., Verma, M., Surampalli, R., 2015. Triclosan: current status, occurrence, environmental risks and bioaccumulation potential. *Int. J. Environ. Res. Public Health* 12, 5657–5684. <https://doi.org/10.3390/ijerph120505657>.

Dranguet, P., Cosio, C., Le Faucheur, S., Beauvais-Flück, R., Freiburghaus, A., Worms, I.A.M., Petit, B., Civic, N., Docquier, M., Slaveykova, V.I., 2017. Transcriptomic approach for assessment of the impact on microalga and macrophyte of in-situ exposure in river sites contaminated by chlor-alkali plant effluents. *Water Res.* 121, 86–94. <https://doi.org/10.1016/j.watres.2017.05.020>.

EFSA Scientific Committee, Hardy, A., Benford, D., Halldorsson, T., Jeger, M.J., Knutsen, K.H., More, S., Mortensen, A., Naegeli, H., Noteborn, H., Ockleford, C., Ricci, A., Rychen, G., Silano, V., Solecki, R., Turck, D., Aerts, M., Bodin, L., Davis, A., Edler, L., Gundert-Remy, U., Sand, S., Slob, W., Böttch, B., Abraham, J.C., Marques, D.C., Kass, G., Schlatter, J.R., 2017. Update: use of the benchmark dose approach in risk assessment. *EFSA J.* 15. <https://doi.org/10.2903/j.efsa.2017.4658>.

Eriksson, K.M., Johansson, C.H., Fihlman, V., Grehn, A., Sanli, K., Andersson, M.X., Blanck, H., Arrhenius, Å., Sircar, T., Backhaus, T., 2015. Long-term effects of the antibacterial agent triclosan on marine periphyton communities: toxicity of triclosan to marine periphyton communities. *Environ. Toxicol. Chem.* 34, 2067–2077. <https://doi.org/10.1002/etc.3030>.

Franz, S., Altenburger, R., Heilmeyer, H., Schmittjansen, M., 2008. What contributes to the sensitivity of microalgae to triclosan? *Aquat. Toxicol.* 90, 102–108. <https://doi.org/10.1016/j.aquatox.2008.08.003>.

Gündel, U., Kalkhof, S., Zitzkat, D., von Bergen, M., Altenburger, R., Küster, E., 2012. Concentration–response concept in ecotoxicoproteomics: effects of different phenanthrene concentrations to the zebrafish (*Danio rerio*) embryo proteome. *Ecotoxicol. Environ. Saf.* 76, 11–22. <https://doi.org/10.1016/j.ecoenv.2011.10.010>.

Haas, R., Zelezniak, A., Iacovacci, J., Kamrad, S., Townsend, S., Ralsler, M., 2017. Designing and interpreting ‘multi-omic’ experiments that may change our understanding of biology. *Curr. Opin. Syst. Biol.* 6, 37–45. <https://doi.org/10.1016/j.coisb.2017.08.009>.

Haider, S., Pal, R., 2013. Integrated analysis of transcriptomic and proteomic data. *Curr. Genomics* 14, 91–110. <https://doi.org/10.2174/1389202911314020003>.

Jamers, A., Blust, R., De Coen, W., Griffin, J.L., Jones, O.A.H., 2013. An omics based assessment of cadmium toxicity in the green alga *Chlamydomonas reinhardtii*. *Aquat. Toxicol.* 126, 355–364. <https://doi.org/10.1016/j.aquatox.2012.09.007>.

Kanehisa, M., 2000. KEGG: Kyoto encyclopedia of genes and genomes. *Nucleic Acids Res.* 28, 27–30. <https://doi.org/10.1093/nar/28.1.27>.

Larras, F., Billoir, E., Baillard, V., Siberchicot, A., Scholz, S., Wubet, T., Tarkka, M., Schmitt-Jansen, M., Delignette-Muller, M.-L., 2018. DRomics: a turnkey tool to support the use of the dose–response framework for omics data in ecological risk assessment. *Environ. Sci. Technol.* 52, 14461–14468. <https://doi.org/10.1021/acs.est.8b04752>.

Machado, M.D., Soares, E.V., 2019. Sensitivity of freshwater and marine green algae to three compounds of emerging concern. *J. Appl. Phycol.* 31, 399–408. <https://doi.org/10.1007/s10811-018-1511-5>.

McMurry, L., Oethinger, M., Levy, S., 1998. Triclosan targets lipid synthesis. *Nature* 394, 531–532. <https://doi.org/10.1038/28970>.

Misra, B.B., Langefeld, C., Olivier, M., Cox, L.A., 2019. Integrated omics: tools, advances and future approaches. *J. Mol. Endocrinol.* R21–R45. <https://doi.org/10.1530/JME-18-0055>.

Moisset, S., Tiam, S.K., Feurtet-Mazel, A., Morin, S., Delmas, F., Mazzella, N., Gonzalez,

- P., 2015. Genetic and physiological responses of three freshwater diatoms to realistic diuron exposures. *Environ. Sci. Pollut. Res. - Int.* 22, 4046–4055. <https://doi.org/10.1007/s11356-014-3523-2>.
- Pan, C.-G., Peng, F.-J., Shi, W.-J., Hu, L.-X., Wei, X.-D., Ying, G.-G., 2018. Triclosan-induced transcriptional and biochemical alterations in the freshwater green algae *Chlamydomonas reinhardtii*. *Ecotoxicol. Environ. Saf.* 148, 393–401. <https://doi.org/10.1016/j.ecoenv.2017.10.011>.
- Pesce, S., Beguet, J., Rouard, N., Devers-Lamrani, M., Martin-Laurent, F., 2013. Response of a diuron-degrading community to diuron exposure assessed by real-time quantitative PCR monitoring of phenylurea hydrolase A and B encoding genes. *Appl. Microbiol. Biotechnol.* 97, 1661–1668. <https://doi.org/10.1007/s00253-012-4318-3>.
- Pillai, S., Behra, R., Nestler, H., Suter, M.J.-F., Sigg, L., Schirmer, K., 2014. Linking toxicity and adaptive responses across the transcriptome, proteome, and phenotype of *Chlamydomonas reinhardtii* exposed to silver. *Proc. Natl. Acad. Sci.* 111, 3490–3495. <https://doi.org/10.1073/pnas.1319388111>.
- Pinckney, J.L., Thompson, L., Hylton, S., 2017. Triclosan alterations of estuarine phytoplankton community structure. *Mar. Pollut. Bull.* 119, 162–168. <https://doi.org/10.1016/j.marpolbul.2017.03.056>.
- Pinu, F.R., Beale, D.J., Paten, A.M., Kouremenos, K., Swarup, S., Schirra, H.J., Wishart, D., 2019. Systems biology and multi-omics integration: viewpoints from the metabolomics research community. *Metabolites* 9, 76. <https://doi.org/10.3390/metabo9040076>.
- Riedl, J., Schreiber, R., Otto, M., Heilmeyer, H., Altenburger, R., Schmitt-Jansen, M., 2015. Metabolic effect level index links multivariate metabolic fingerprints to ecotoxicological effect assessment. *Environ. Sci. Technol.* 49, 8096–8104. <https://doi.org/10.1021/acs.est.5b01386>.
- Sarkar, N., Lemaire, S., Wu-Scharf, D., Issakidis-Bourguet, E., Cerutti, H., 2005. Functional specialization of *Chlamydomonas reinhardtii* cytosolic thioredoxin h1 in the response to alkylation-induced DNA damage. *Eukaryot. Cell* 4, 262–273. <https://doi.org/10.1128/EC.4.2.262-273.2005>.
- Schüttler, A., Reiche, K., Altenburger, R., Busch, W., 2017. The transcriptome of the zebrafish embryo after chemical exposure: a meta-analysis. *Toxicol. Sci.* 157, 291–304. <https://doi.org/10.1093/toxsci/kfx045>.
- Schüttler, A., Altenburger, R., Ammar, M., Bader-Blukott, M., Jakobs, G., Knapp, J., Krüger, J., Reiche, K., Wu, G.-M., Busch, W., 2019. Map and model—moving from observation to prediction in toxicogenomics. *GigaScience* 8. <https://doi.org/10.1093/gigascience/giz057>.
- Singer, H., Müller, S., Tixier, C., Pillonel, L., 2002. Triclosan: occurrence and fate of a widely used biocide in the aquatic environment: field measurements in wastewater treatment plants, surface waters, and Lake Sediments. *Environ. Sci. Technol.* 36, 4998–5004. <https://doi.org/10.1021/es025750i>.
- Smetanová, S., Riedl, J., Zitzkat, D., Altenburger, R., Busch, W., 2015. High-throughput concentration-response analysis for omics datasets: concentration-response analysis for omics datasets. *Environ. Toxicol. Chem.* 34, 2167–2180. <https://doi.org/10.1002/etc.3025>.
- Sotton, B., Paris, A., Le Manach, S., Blond, A., Duval, C., Qiao, Q., Catherine, A., Combes, A., Pichon, V., Bernard, C., Marie, B., 2019. Specificity of the metabolic signatures of fish from cyanobacteria rich lakes. *Chemosphere* 226, 183–191. <https://doi.org/10.1016/j.chemosphere.2019.03.115>.
- Tato, T., Beiras, R., 2019. The use of the marine microalga *tisochrysis lutea* (T-iso) in standard toxicity tests; comparative sensitivity with other test species. *Front. Mar. Sci.* 6. <https://doi.org/10.3389/fmars.2019.00488>.
- The UniProt Consortium, 2019. UniProt: a worldwide hub of protein knowledge. *Nucleic Acids Res.* 47, D506–D515. <https://doi.org/10.1093/nar/gky1049>.
- Thomas, R.S., Allen, B.C., Nong, A., Yang, L., Bermudez, E., Clewell, H.J., Andersen, M.E., 2007. A method to integrate benchmark dose estimates with genomic data to assess the functional effects of chemical exposure. *Toxicol. Sci.* 98, 240–248. <https://doi.org/10.1093/toxsci/kfm092>.
- Vogs, C., Altenburger, R., 2016. Time-dependent effects in algae for chemicals with different adverse outcome pathways: a novel approach. *Environ. Sci. Technol.* 50, 7770–7780. <https://doi.org/10.1021/acs.est.6b00529>.
- von der Ohe, P.C., Schmitt-Jansen, M., Slobodnik, J., Brack, W., 2012. Triclosan—the forgotten priority substance? *Environ. Sci. Pollut. Res. - Int.* 19, 585–591. <https://doi.org/10.1007/s11356-011-0580-7>.
- Wang, P., Xia, P., Yang, J., Wang, Z., Peng, Y., Shi, W., Villeneuve, D.L., Yu, H., Zhang, X., 2018. A reduced transcriptome approach to assess environmental toxicants using zebrafish embryo test. *Environ. Sci. Technol.* 52, 821–830. <https://doi.org/10.1021/acs.est.7b04073>.
- Xin, X., Huang, G., An, C., Raina-Fulton, R., Weger, H., 2019. Insights into long-term toxicity of triclosan to freshwater green algae in Lake Erie. *Environ. Sci. Technol.* 53, 2189–2198. <https://doi.org/10.1021/acs.est.9b00259>.
- Zhang, X., Xia, P., Wang, P., Yang, J., Baird, D.J., 2018. Omics advances in ecotoxicology. *Environ. Sci. Technol.* 52, 3842–3851. <https://doi.org/10.1021/acs.est.7b06494>.